HAL open science

Exploration of stable compounds, crystal structures, and superconductivity in the Be-H system

Shuyin Yu, Qingfeng Zeng, Artem R. Oganov, Chaohao Hu, Gilles Frapper, Litong Zhang

To cite this version:

Shuyin Yu, Qingfeng Zeng, Artem R. Oganov, Chaohao Hu, Gilles Frapper, et al.. Exploration of stable compounds, crystal structures, and superconductivity in the Be-H system. AIP Advances, 2014, 4 (10), 10.1063/1.4898145 . hal-01324799

HAL Id: hal-01324799

https://hal.science/hal-01324799v1

Submitted on 23 Sep 2021

HAL is a multi-disciplinary open access archive for the deposit and dissemination of scientific research documents, whether they are published or not. The documents may come from teaching and research institutions in France or abroad, or from public or private research centers.

L'archive ouverte pluridisciplinaire **HAL**, est destinée au dépôt et à la diffusion de documents scientifiques de niveau recherche, publiés ou non, émanant des établissements d'enseignement et de recherche français ou étrangers, des laboratoires publics ou privés.

Distributed under a Creative Commons Attribution 4.0 International License

AIP Advances

Exploration of stable compounds, crystal structures, and superconductivity in the Be-H system

Cite as: AIP Advances **4**, 107118 (2014); https://doi.org/10.1063/1.4898145
Submitted: 09 July 2014 . Accepted: 30 September 2014 . Published Online: 10 October 2014

Shuyin Yu, Qingfeng Zeng, Artem R. Oganov, Chaohao Hu, Gilles Frapper, Litong Zhang, et al.

View Online Export Citation CrossMark

ARTICLES YOU MAY BE INTERESTED IN

Metallization and superconductivity of BeH_2 under high pressure
The Journal of Chemical Physics **140**, 124707 (2014); https://doi.org/10.1063/1.4869145

High-temperature superconductivity in alkaline and rare earth polyhydrides at high pressure: A theoretical perspective
The Journal of Chemical Physics **150**, 050901 (2019); https://doi.org/10.1063/1.5079225

The metallization and superconductivity of dense hydrogen sulfide
The Journal of Chemical Physics **140**, 174712 (2014); https://doi.org/10.1063/1.4874158

© 2014 Author(s).

AIP ADVANCES **4**, 107118 (2014)

Exploration of stable compounds, crystal structures, and superconductivity in the Be-H system

Shuyin Yu,[1,a] Qingfeng Zeng,[1] Artem R. Oganov,[2,3,4] Chaohao Hu,[5] Gilles Frapper,[6] and Litong Zhang[1]

[1]*Science and Technology on Thermostructural Composite Materials Laboratory, School of Materials Science and Engineering, Northwestern Polytechnical University, Xi'an, Shaanxi 710072, PR China*

[2]*Department of Geosciences, Center for Materials by Design, and Institute for Advanced Computational Science, State University of New York, Stony Brook, NY 11794-2100, USA*

[3]*Moscow Institute of Physics and Technology, Dolgoprudny, Moscow Region 141700, Russia*

[4]*School of Materials Science and Engineering, Northwestern Polytechnical University, Xi'an, Shaanxi 710072, PR China*

[5]*School of Materials Science and Engineering, Guilin University of Electronic Technology, Guilin 541004, People's Republic of China*

[6]*IC2MP UMR 7285, Université de Poitiers - CNRS, Poitiers 86022, France*

(Received 9 July 2014; accepted 30 September 2014; published online 10 October 2014)

Using first-principles variable-composition evolutionary methodology, we explored the high-pressure structures of beryllium hydrides between 0 and 400 GPa. We found that BeH_2 remains the only stable compound in this pressure range. The pressure-induced transformations are predicted as $Ibam \rightarrow P\bar{3}m1 \rightarrow R\bar{3}m \rightarrow Cmcm \rightarrow P4/nmm$, which occur at 24, 139, 204 and 349 GPa, respectively. $P\bar{3}m1$ and $R\bar{3}m$ structures are layered polytypes based on close packings of H atoms with Be atoms filling all octahedral voids in alternating layers. *Cmcm* and *P4/nmm* contain two-dimensional triangular networks with each layer forming a kinked slab in the *ab*-plane. $P\bar{3}m1$ and $R\bar{3}m$ are semiconductors while *Cmcm* and *P4/nmm* are metallic. We have explored superconductivity of both metal phases, and found large electron-phonon coupling parameters of λ=0.63 for *Cmcm* with a T_c of 32.1-44.1 K at 250 GPa and λ=0.65 for *P4/nmm* with a T_c of 46.1-62.4 K at 400 GPa. The dependence of T_c on pressure indicates that T_c initially increases to a maximum of 45.1 K for *Cmcm* at 275 GPa and 97.0 K for *P4/nmm* at 365 GPa, and then decreases with increasing pressure for both phases. © *2014 Author(s). All article content, except where otherwise noted, is licensed under a Creative Commons Attribution 3.0 Unported License.* [http://dx.doi.org/10.1063/1.4898145]

INTRODUCTION

The search for new high-temperature superconductors has attracted great enthusiasm in both fundamental and applied research. Owing to its low mass and high electron density, "metallic hydrogen" has been predicted to possess a high superconducting transition temperature (T_c > 200 K).[1–3] However, hydrogen remains insulating at extremely high pressure (>320 GPa[4]), which are too high for any applications. Another feasible method of obtaining the properties of metallic hydrogen is to form hydrogen-rich alloys with other elements.[5] Due to "chemical precompression," the pressure of metallization may be reduced significantly.

Inspired by the elusive state of matter, theoretical and experimental research has made considerable progress towards exploring superconductivity in hydrogen-rich compounds, e.g. for group IVa hydrides, calculations predicted that SiH_4,[6–9] $SiH_4(H_2)_2$,[10] GeH_4,[11–13] SnH_4[14,15] and PbH_4[16] may become superconductors at high (yet lower than pure H) pressure. The origin of high-pressure superconductivity can be derived from the particular "H_2" units, which are a feature common to

[a]Electronic address: yushuyin2014@gmail.com

 ©Author(s) 2014

hydrides of alkali metals,[17] alkaline earth metals[18,19] and group IVa elements.[12,15] Experiments suggested metallization of SiH_4 at ~60 GPa[20] and its superconducting transition temperature (T_c) is 17 K at 96 and 120 GPa,[21] though debates remain. In addition, the superconductivity of group IIIa hydrides (BH,[22] AlH_3[23,24] and GaH_3[25]) and alkaline earth metal hydrides (CaH_n,[26] SrH_n[19] and BaH_n[18]) have also been extensively explored.

Beryllium hydrides can be an interesting subject of study, because low atomic mass of Be may lead to very high T_c values. The only known beryllium hydride is BeH_2. The ground-state structure of BeH_2 is body-centered orthorhombic with *Ibam*[27] symmetry. At ambient conditions, BeH_2 is an insulator with a pronounced band gap of 5.5 eV.[28] Vajeeston *et al.*[29] proposed that BeH_2 undergoes a series of phase transitions $\alpha \rightarrow \beta \rightarrow \gamma \rightarrow \delta \rightarrow \epsilon$ at pressures of 7, 51, 87 and 98 GPa, respectively, and reported that BeH_2 remains insulating up to 100 GPa. Zhang *et al.*[30] systematically investigated the pressure-induced metallization of alkaline earth hydrides, and found the metallization pressure of *Pnma*-BeH_2 to be greater than 300 GPa. Wang *et al.*[31] predicted that BeH_2 reaches a metallic state by a $R\bar{3}m \rightarrow Cmcm$ phase transition, instead of a direct band gap closure in $R\bar{3}m$ phase.

METHOD

First-principles variable-composition evolutionary simulations were performed at 0, 50, 100, 150, 200, 250, 300 and 400 GPa using the USPEX code,[32–35] which has the capability of discovering possible stoichiometries and the corresponding stable and metastable structures at given pressure-temperature conditions, and has successfully predicted a large number of stable structures.[36–38] The initial generation of structures and compositions was produced randomly with the use of space groups picked randomly from the total list of 230 groups. 50% of the lowest-enthalpy structures were used as parents for the next generation. In addition, 20% of structures in each new generation were produced by lattice mutation, 15% by atomic transmutation and 15% were produced randomly. Each generation contained 60 structures and runs proceeded for up to 50 generations.

The underlying structure relaxations were carried out using the Vienna *Ab-initio* Simulation Package (VASP) code,[39] in the framework of density functional theory (DFT)[40,41] within the Perdew Burke Ernzerhof generalized gradient approximation (PBE-GGA).[42] The frozen all-electron projected augmented wave approach (PAW)[43] was adopted to describe the core electrons and their effects on valence orbitals. A plane-wave kinetic energy cutoff of 600 eV and dense Monkhorst-Pack k-point grids[44] with a resolution higher than $2\pi \times 0.06$ Å^{-1} were used for all structures. The most stable structures were studied further at increased accuracy using a reciprocal-space grid better than $2\pi \times 0.03$ Å^{-1}.

Phonon calculations were carried out using the supercell approach as implemented in the PHONOPY code.[45] Electron-phonon coupling (EPC) calculations were explored using the pseudopotential plane-wave method within PBE-GGA, as implemented in the Quantum-Espresso package.[46] In these calculations, we used the kinetic energy cutoff of 60 Ry and Monkhorst-Pack k-point grids of $20 \times 20 \times 12$ for the *Cmcm* phase and $16 \times 16 \times 8$ for the *P4/nmm* phase with a Methfessel-Paxton[47] smearing factor of 0.05 Ry. Additionally, q-meshes of $5 \times 5 \times 3$ for *Cmcm* and $4 \times 4 \times 2$ for *P4/nmm* were used to calculate the electron-phonon coupling matrix elements, respectively. We used the Allen-Dynes-modified McMillan equation[48] to estimate T_c, as follows:

$$T_c = \frac{\omega_{\log}}{1.2} \exp\left[-\frac{1.04(1+\lambda)}{\lambda - \mu^*(1+0.62\lambda)}\right] \tag{1}$$

where ω_{log} is the logarithmic average frequency, λ is the electron-phonon coupling constant and μ^* is the Coulomb pseudopotential, which is assumed to be between 0.10-0.13.[5]

RESULTS AND DISCUSSIONS

Fig. 1 shows the convex hull phase diagrams for the Be-H system at selected pressures. The ground-state enthalpy of formation ΔH_f is defined as $\Delta H_f(Be_xH_y) = \Delta H(Be_xH_y) - x\Delta H(Be) - y\Delta H(H)$. A compound is thermodynamically stable if it has lower enthalpy than any isochemical

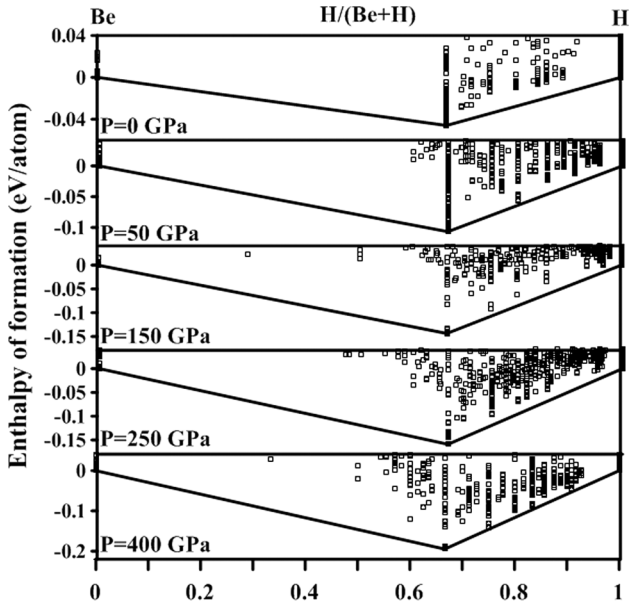

FIG. 1. Convex hull phase diagrams for the Be-H system at 0, 50, 150, 250 and 400 GPa.

mixture of the elements or other compounds. Such stable compounds form the convex hull. Based on our evolutionary searches, elemental Be adopts the $P6_3/mmc$ structure below 390 GPa and *bcc* $Im\bar{3}m$ structure above 390 GPa. Our findings are in good agreement with previous calculations.[49] Hydrogen undergoes a series of phase transitions: $P6_3/m$ (P < 105 GPa), $C2/c$ (105 < P < 207 GPa), $Cmca$-12 (270 < P < 385 GPa), $Cmca$ (P > 385 GPa),[50] in addition to the experimentally known *Ibam*,[27] structure, we found a series of pressure-induced structural transformations ($Ibam \rightarrow P\bar{3}m1 \rightarrow R\bar{3}m \rightarrow Cmcm \rightarrow P4/nmm$) with increasing pressure. Notably, we did not find other stable compounds besides BeH_2 over the entire pressure range 0-400 GPa. The detailed structural parameters of these predicted phases are summarized in Table I.

At ambient conditions, BeH_2 crystallizes in the orthorhombic *Ibam* structure. This structure consists of a three-dimensional network of distorted tetrahedra with Be atoms sitting at the center of the tetrahedra and H atoms at the corner in a bridged position between two Be atoms. The orthorhombic phase transforms to a CdI_2-type structure ($P\bar{3}m1$; Fig. 2(a)) at 24 GPa, then it transforms to a related $CdCl_2$-type structure ($R\bar{3}m$; Fig. 2(b)) at 139 GPa (Fig. 3(a)). Both structures are made

TABLE I. Optimized structural parameters for the predicted BeH_2 structures at selected pressures.

Pressure			Lattice parameters		Wyckoff positions			
(GPa)	Space group	No.	(Å, deg)	Atom	Sites	x	y	z
50	$P\bar{3}m1$	164	a = 2.085	Be	*1a*	0	0	0
			c = 3.104	H	*2d*	0.667	0.333	0.721
150	$R\bar{3}m$	166	a = 1.886	Be	*1b*	0	0	0.5
			c = 8.316	H	*2c*	0	0	0.732
250	*Cmcm*	63	a = 1.796	Be	*4c*	0	0.139	0.75
			b = 5.503	H1	*4b*	0	0.5	1
			c = 2.840	H2	*4c*	0	0.819	0.75
400	*P4/nmm*	129	a = 1.906	Be	*2c*	0.5	0	0.707
			c = 3.240	H1	*2a*	0	0	0
				H2	*2c*	0.5	0	0.327

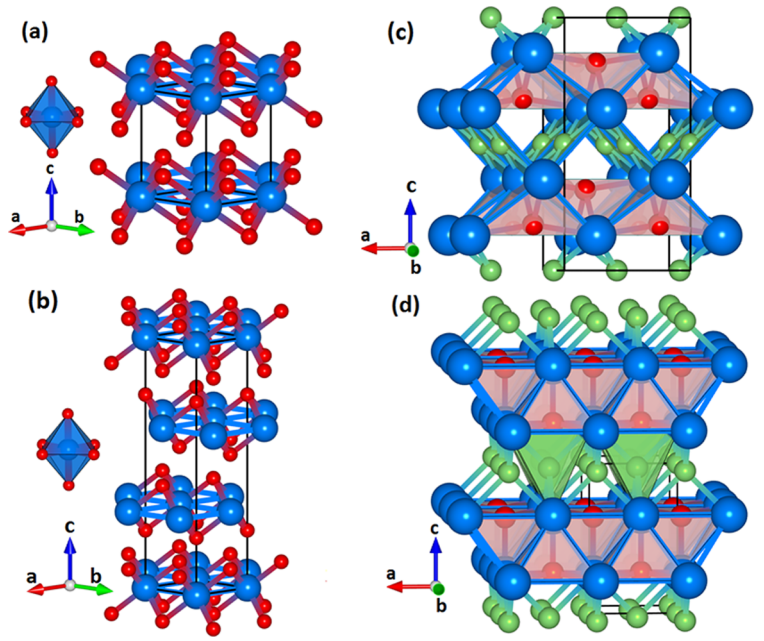

FIG. 2. Extended crystal structures of solid BeH_2 for (a) the $P\bar{3}m1$ structure at 50 GPa; (b) the $R\bar{3}m$ structure at 150 GPa; (c) the *Cmcm* structure at 250 GPa; and (d) the *P4/nmm* structure at 400 GPa. The large blue spheres represent Be atoms, while the small red and green spheres indicate two symmetrically inequivalent H atoms.

of layers of edge-sharing BeH_6-octahedra, but stacking sequences of these layers are different. The shortest interlayer H-H distances decrease from 1.83 Å at 50 GPa to 1.51 Å at 150 GPa (Fig. 3(b)).

We found a similar high-pressure structure in the B-H system:[22] at P > 168 GPa, the *P6/mmm*-BH structure is the most stable phase, and may be described as stacking BH-layers with planar closely-packed arrays of boron atoms. On-top H atoms locate symmetrically between the boron layers. Note that if one assigns a formal charge of -1 to H (hydride-like), both the boron atoms in BH and beryllium atoms in BeH_2 have a formal ns^2 valence electron configuration. Notably, the structural transformation from *Ibam* to $P\bar{3}m1$ is accompanied by a large density jump of 9.81% while only 0.79% increase occurs at the transition from $P\bar{3}m1$ to $R\bar{3}m$ (Fig. 3(b)). The structures in Ref. 27 are metastable with respect to the $P\bar{3}m1$ structure.

At 204 GPa, the layered $R\bar{3}m$ structure transforms into an orthorhombic *Cmcm* structure (Fig. 2(c)). In this structure, Be atoms are coordinated by eight hydrogens, whereas hydrogens are in the fourfold coordination (H1 atoms - in planar square coordination, H2 atoms - in tetrahedral coordination). Note that H1 atoms form flat pure-hydrogen rectangular layers with shortest H-H distance of 1.42 Å at 250 GPa. The tetragonal *P4/nmm* structure (PbClF-type) becomes stable at 349 GPa. In this structure, Be atoms are coordinated by nine hydrogen atoms (forming a capped tetragonal antiprism); H1 atoms are in a fourfold (planar square) coordination and H2 atoms in a fivefold (square pyramid) coordination. The structure can be viewed as layered, with double layers formed by Be and H2 atoms, alternating with square layers formed by H1 atoms. The Be-Be distances at 400 GPa are 1.901 and 1.906 Å within the double layers, and 2.328 Å between these layers, reinforcing cohesion of the highly delocalized covalent three-dimensional BeH_2 structure. The shortest H-H distance is between H1 atoms, i.e. in the pure-hydrogen square layer - at 400 GPa this distance is 1.345 Å. At such distances overlap of atomic orbitals is strong enough to make the material metallic. This is very similar to the *Pbcn*-SiH_4[9] with the closest H-H distance of 1.35 Å.

Fig. 4 shows electronic densities of states (DOS) for the $P\bar{3}m1$ and $R\bar{3}m$ structures, from which it can be clearly seen that both structures are insulting. As we know, GW approximation can precisely estimate the materials band gaps in contrast to the GGA and LDA methods. For the $P\bar{3}m1$ and $R\bar{3}m$ phases, the gaps are 3.12 eV at 50 GPa and 1.80 eV at 150 GPa, respectively, indicating that both structures can be viewed as wide band gap semiconductors. In addition, it is clear that there is

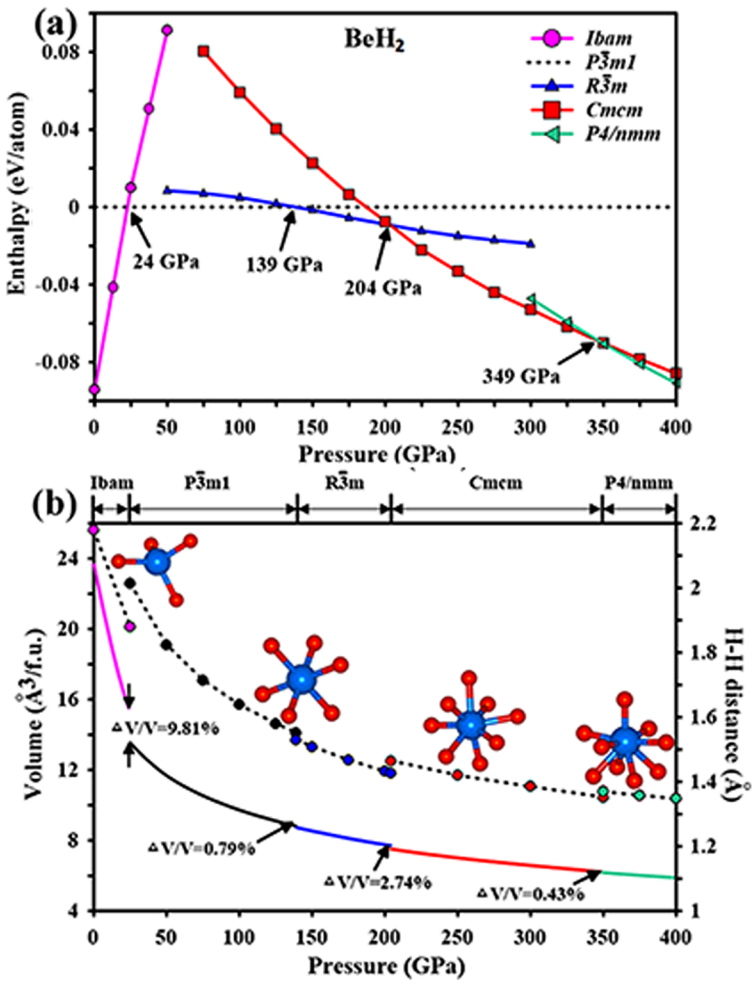

FIG. 3. (a) Enthalpy per atom for various BeH_2 structures as a function of pressure with the $P\bar{3}m1$ structure taken as the reference; (b) Computed equations of state of BeH_2 (solid lines) and shortest H-H distance (dotted lines).

substantial hybridization of the Be-*p* states and H-*s* states, suggesting large degree of covalency. The covalent bonds are mainly from the intralayer BeH_6 octahedra while the interlayer interactions are mainly van der Waals forces.

Fig. 5 shows the band structures, partial DOS and electron localization function (ELF) for the *Cmcm* phase at 250 GPa and *P4/nmm* phase at 400 GPa, respectively. The band structures reveal that both structures are metallic with several bands crossing the Fermi level, and a pseudogap. The dispersed valence and conduction bands near the Fermi level signify a relatively large DOS at the Fermi level (0.098 and 0.107 electrons/eV/f.u., respectively), which may favor superconducting behavior. The valence band widths are greater than in the low-pressure phases, which indicates enhanced electron delocalization, thus, more electrons participate in bonding interactions, which promotes structural stability.

Distributions of the electron localization function (ELF) reveal electron accumulation on the H atoms. For the *P4/nmm* phase, the ELF between H atoms in the square H-layer is close to 0.5 (Fig. 5(e)), which equals to the value for the electron gas. This indicates that the square H-layer is metallic, which we think it is the origin of the superconductivity. In the *Cmcm* phase, Bader[51] analysis reveals that Be atoms have charge +1.58 and the charges of H1 and H2 atoms are -0.82 and -0.76, respectively. The charges of Be, H1 and H2 atoms of the *P4/nmm* phase are +1.57, -0.94 and -0.63, respectively. It is obvious that there are large charge transfer from Be atoms to H atoms

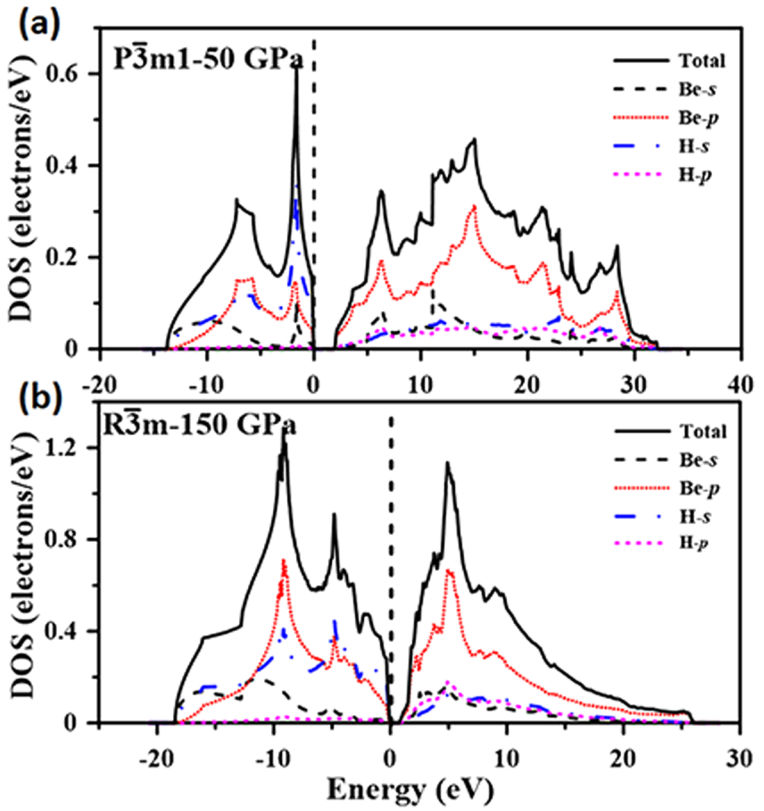

FIG. 4. Total and Partial density of states (DOS) for the (a) $P\bar{3}m1$ phase at 50 GPa and (b) $R\bar{3}m$ phase at 150 GPa.

for both structures, indicating the ionic character of the bonds. Together with the DOS and ELF analysis, the bonding nature can be characterized as mixed metallic, covalent and ionic bonds.

The calculated phonon spectra for the *Cmcm* and *P4/nmm* phases establish dynamical stability, as there are no imaginary phonon frequencies anywhere in the Brillouin zone (Fig. 6). We further explored the superconductivity for both structures by performing electron-phonon coupling (EPC) calculations. For the *Cmcm* structure at 250 GPa, the electron-phonon coupling parameter λ is 0.63, indicative of quite strong EPC. Using the calculated ω_{log} of 1670.7 K and the commonly accepted values of the Coulomb pseudopotential μ^* (0.1-0.13),[5] we obtained T_c in the range of 32.1-44.1 K using the modified Allen-Dynes-modified McMillan equation.[48] Our results are similar to those of Wang *et al.*,[31] the differences being due to different pseudopotentials. From Fig. 7(c), it is clear that T_c of the *Cmcm* structure first increases and then decreases with increasing pressure, and reaches a maximum (45.1 K) at ~275 GPa.

Fig. 7 shows the total and partial phonon density of states together with the Eliashberg phonon spectral function $\alpha^2F(\omega)$ and electron-phonon integral $\lambda(\omega)$ as a function of frequency for the *P4/nmm* structure at 400 GPa. Low-frequency (<35 THz) vibrations are mostly related to Be atoms, while higher-frequency (>45 THz) modes mainly come from the vibration of H1 and H2 atoms. At 400 GPa, The calculated EPC parameter λ is 0.65, indicating rather strong EPC in the *P4/nmm* structure. Using the calculated ω_{log} of 2170 K and μ^* (0.1-0.13), we obtained T_c in the range of 46.1-62.4 K. The vibrations of Be below 35 THz contribute about 44.3% of total λ, while the vibrations of H1 and H2 above 45 THz contribute about 55.7% with no obvious difference between H1 and H2 vibrations to λ. In addition, the pressure dependence of T_c displays the same trend as observed in the *Cmcm* phase and reaches a maximum of 97.0 K at 365 GPa. This is one of the highest T_c values predicted in the literature. Note that the Allen-Dynes formula is expected to be reliable when λ is less than 1–1.5,[52] which is the case here.

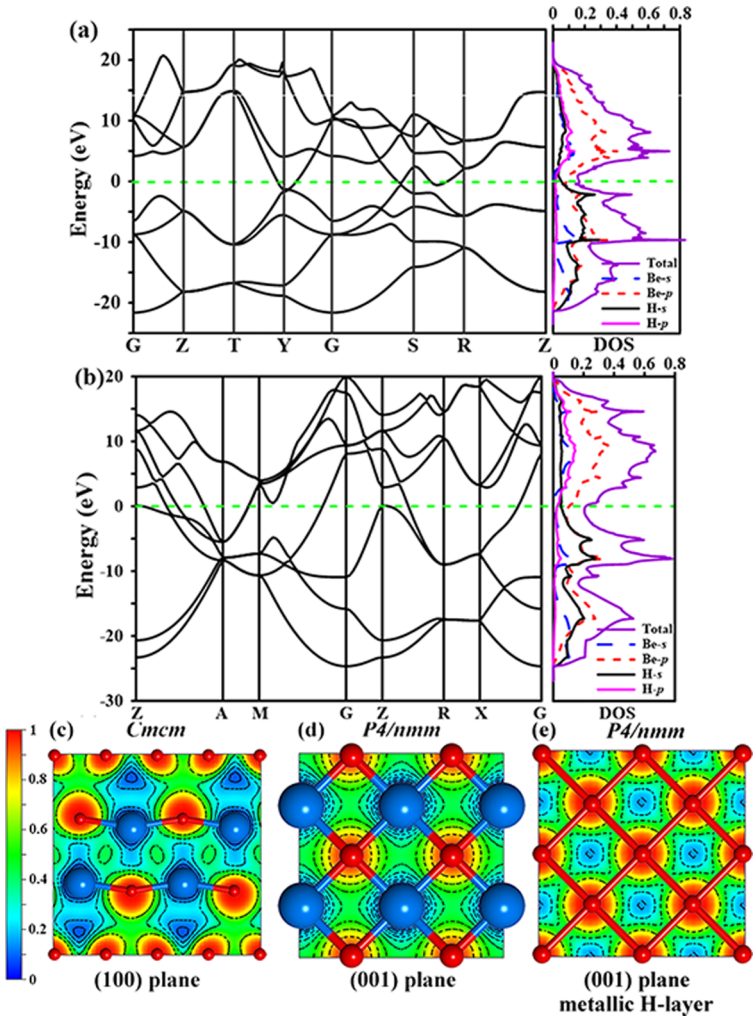

FIG. 5. (a) and (b) band structures and partial DOS for *Cmcm* phase at 250 GPa and *P4/nmm* phase at 400 GPa, respectively; (c), (d) and (e) electron localization function (ELF) through specific surfaces.

CONCLUSIONS

In summary, using variable-composition evolutionary simulations for crystal structure prediction, we investigated the high-pressure phases of solid beryllium hydrides in the pressure range of 0-400 GPa. BeH_2 is found to be the only stable beryllium hydride. The pressure-induced transformations are predicted to be $Ibam \rightarrow P\bar{3}m1 \rightarrow R\bar{3}m \rightarrow Cmcm \rightarrow P4/nmm$, which occur at 24, 139, 204 and 349 GPa, respectively. The layered $P\bar{3}m1$ and $R\bar{3}m$ structures belong to the well-known CdI_2 and $CdCl_2$ types, respectively. The *Cmcm* and *P4/nmm* phases contain 8- and 9-coordinate Be atoms, respectively, and layers of H atoms with short H-H distances, responsible for metallic conductivity. The entire phase transformations are first-order with volume shrinkage values of 9.81%, 0.79%, 2.71% and 0.43%, respectively. The $P\bar{3}m1$ and $R\bar{3}m$ structures are semiconductors while the *Cmcm* and *P4/nmm* phases are metallic. Electron-phonon coupling calculations show that the *Cmcm* and *P4/nmm* structures are phonon-mediated superconductors, with large electron-phonon coupling parameters of 0.63 for the *Cmcm* phase with a T_c of 32.1-44.1 K at 250 GPa and 0.65 for the *P4/nmm* phase with a T_c of 46.1-62.4 K at 400 GPa. Dependence of T_c on pressure indicates that T_c will increase initially to a maximum value of 45.1 K for the *Cmcm* phase at 275 GPa and 97.0 K for the *P4/nmm* phase at 365 GPa, respectively, and then decrease with increasing pressure for both structures.

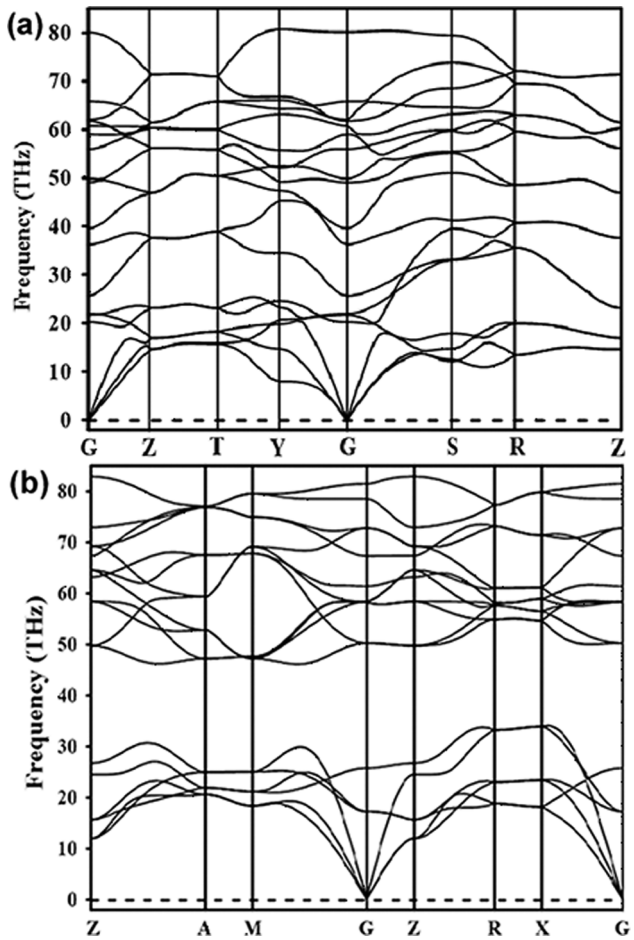

FIG. 6. Calculated phonon spectra along selected high symmetry points for (a) the *Cmcm* phase at 250 GPa and (b) *P4/nmm* phase at 400 GPa.

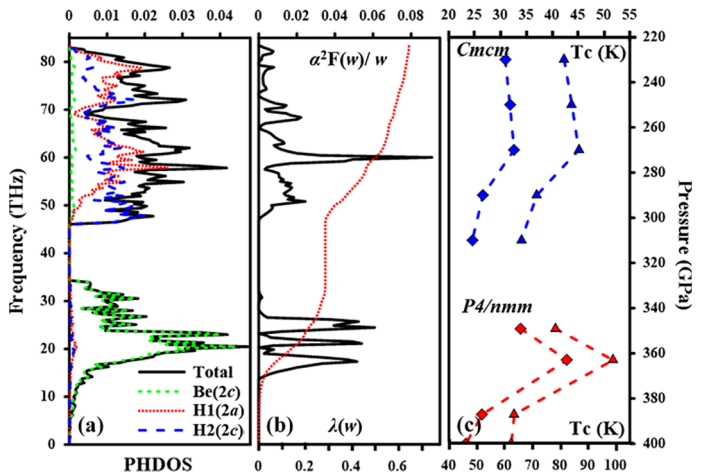

FIG. 7. (a) Total and partial phonon density of states (PDOS) for *P4/nmm* phase; (b) Eliashberg phonon spectral function $\alpha^2F(\omega)$ and electron-phonon integral $\lambda(\omega)$ as a function of frequency at 400 GPa; and (c) calculated superconducting transition temperature (T_c) *vs* pressure for *Cmcm* and *P4/nmm* phases, triangles and squares represent $\mu^* = 0.1$ and 0.13, respectively.

We thank the Natural Science Foundation of China (Grants No. 51372203, No. 11164005 and No. 51332004), the National Basic Research Program of China (973 Program, Grant No. 2014CB643703), the Basic Research Foundation of NWPU (Grant No. JCY20130114), the Foreign Talents Introduction and Academic Exchange Program (Grant No. B08040), the National Science Foundation (Grants No. EAR-1114313 and No. DMR-1231586), DARPA (Grants No. W31P4Q1310005 and No. W31P4Q1210008), and the Government of the Russian Federation (Grant No. 14.A12.31.0003) for financial support. The authors also acknowledge the High Performance Computing Center of NWPU, Shanghai Supercomputer Centre, and the National Supercomputing Center in Shenzhen and the GENCI-CINES (France) for the allocation of computing time on their machines.

[1] N. W. Ashcroft, Physical Review Letters **21**, 1748 (1968).
[2] T. Barbee, A. García, and M. L. Cohen, Nature **340**, 369 (1989).
[3] P. Cudazzo, G. Profeta, A. Sanna, A. Floris, A. Continenza, S. Massidda, and E. Gross, Physical Review Letters **100**, 257001 (2008).
[4] P. Loubeyre, F. Occelli, and R. LeToullec, Nature **416**, 613 (2002).
[5] N. Ashcroft, Physical Review Letters **92**, 187002 (2004).
[6] J. Feng, W. Grochala, T. Jaroń, R. Hoffmann, A. Bergara, and N. Ashcroft, Physical Review Letters **96**, 017006 (2006).
[7] Y. Yao, J. Tse, Y. Ma, and K. Tanaka, EPL (Europhysics Letters) **78**, 37003 (2007).
[8] A. Durajski and R. Szczśniak, Modern Physics Letters B **28** (2014).
[9] M. Martinez Canales, A. R. Oganov, Y. Ma, Y. Yan, A. O. Lyakhov, and A. Bergara, Physical Review Letters **102**, 087005 (2009).
[10] A. Durajski *et al.*, Solid State Communications **153**, 26 (2013).
[11] A. Durajski *et al.*, arXiv preprint arXiv:1212.2356, (2012).
[12] G. Gao, A. R. Oganov, A. Bergara, M. Martinez Canales, T. Cui, T. Iitaka, Y. Ma, and G. Zou, Physical Review Letters **101**, 107002 (2008).
[13] Z. Li, W. Yu, and C. Jin, Solid State Communications **143**, 353 (2007).
[14] J. Tse, Y. Yao, and K. Tanaka, Physical Review Letters **98**, 117004 (2007).
[15] G. Gao, A. R. Oganov, P. Li, Z. Li, H. Wang, T. Cui, Y. Ma, A. Bergara, A. O. Lyakhov, and T. Iitaka *et al.*, Proceedings of the National Academy of Sciences **107**, 1317 (2010).
[16] P. Zaleski Ejgierd, R. Hoffmann, and N. Ashcroft, Physical Review Letters **107**, 037002 (2011).
[17] E. Zurek, R. Hoffmann, N. Ashcroft, A. R. Oganov, and A. O. Lyakhov, Proceedings of the National Academy of Sciences **106**, 17640 (2009).
[18] J. Hooper, B. Altintas, A. Shamp, and E. Zurek, The Journal of Physical Chemistry C **117**, 2982 (2013).
[19] J. Hooper, T. Terpstra, A. Shamp, and E. Zurek, The Journal of Physical Chemistry C (2014).
[20] X. J. Chen, V. V. Struzhkin, Y. Song, A. F. Goncharov, M. Ahart, Z. Liu, H. K. Mao, and R. J. Hemley, Proceedings of the National Academy of Sciences **105**, 20 (2008).
[21] M. Eremets, I. Trojan, S. Medvedev, J. Tse, and Y. Yao, Science **319**, 1506 (2008).
[22] C. Hu, A. R. Oganov, Q. Zhu, G. R. Qian, G. Frapper, A. O. Lyakhov, and H. Y. Zhou, Physical Review Letters **110**, 165504 (2013).
[23] I. Goncharenko, M. Eremets, M. Hanfland, J. Tse, M. Amboage, Y. Yao, and I. Trojan, Physical Review Letters **100**, 045504 (2008).
[24] A. Islam, M. Ali, and M. Ali, Physica C: Superconductivity **470**, 403 (2010).
[25] G. Gao, H. Wang, A. Bergara, Y. Li, G. Liu, and Y. Ma, Physical Review B **84**, 064118 (2011).
[26] H. Wang, S. T. John, K. Tanaka, T. Iitaka, and Y. Ma, Proceedings of the National Academy of Sciences **109**, 6463 (2012).
[27] G. S. Smith, Q. C. Johnson, D. K. Smith, D. Cox, R. L. Snyder, R.-S. Zhou, and A. Zalkin, Solid State Communications **67**, 491 (1988).
[28] B. T. Wang, P. Zhang, H. L. Shi, B. Sun, and W. D. Li, The European Physical Journal B **74**, 303 (2010).
[29] P. Vajeeston, P. Ravindran, A. Kjekshus, and H. Fjellvag, Applied physics Letters **84**, 34 (2004).
[30] C. Zhang, X. J. Chen, R. Q. Zhang, and H. Q. Lin, The Journal of Physical Chemistry C **114**, 14614 (2010).
[31] Z. Wang, Y. Yao, L. Zhu, H. Liu, T. Iitaka, H. Wang, and Y. Ma, The Journal of Chemical Physics **140**, 124707 (2014).
[32] A. R. Oganov and C. W. Glass, The Journal of chemical physics **124**, 244704 (2006).
[33] A. R. Oganov, A. O. Lyakhov, and M. Valle, Accounts of chemical research **44**, 227 (2011).
[34] A. O. Lyakhov, A. R. Oganov, H. T. Stokes, and Q. Zhu, Computer Physics Communications **184**, 1172 (2013).
[35] A. R. Oganov, Y. Ma, A. O. Lyakhov, M. Valle, and C. Gatti, Reviews in Mineralogy and Geochemistry **71**, 271 (2010).
[36] Q. Zeng, J. Peng, A. R. Oganov, Q. Zhu, C. Xie, X. Zhang, D. Dong, L. Zhang, and L. Cheng, Physical Review B **88**, 214107 (2013).
[37] W. Zhang, A. R. Oganov, A. F. Goncharov, Q. Zhu, S. E. Boulfelfel, A. O. Lyakhov, E. Stavrou, M. Somayazulu, V. B. Prakapenka, and Z. Konôpková, Science **342**, 1502 (2013).
[38] Q. Zhu, A. R. Oganov, and A. O. Lyakhov, Physical Chemistry Chemical Physics **15**, 7696 (2013).
[39] G. Kresse and J. Furthmüller, Physical Review B **54**, 11169 (1996).
[40] P. Giannozzi, S. De Gironcoli, P. Pavone, and S. Baroni, Physical Review B **43**, 7231 (1991).
[41] S. Baroni, P. Giannozzi, and A. Testa, Physical Review Letters **58**, 1861 (1987).
[42] J. P. Perdew, K. Burke, and M. Ernzerhof, Physical Review Letters **77**, 3865 (1996).
[43] P. E. Blöchl, Physical Review B **50**, 17953 (1994).
[44] H. J. Monkhorst and J. D. Pack, Physical Review B **13**, 5188 (1976).

[45] A. Togo, F. Oba, and I. Tanaka, Physical Review B **78**, 134106 (2008).
[46] P. Giannozzi, S. Baroni, N. Bonini, M. Calandra, R. Car, C. Cavazzoni, D. Ceresoli, G. L. Chiarotti, M. Cococcioni, and I. Dabo *et al.*, Journal of Physics: Condensed Matter **21**, 395502 (2009).
[47] M. Methfessel and A. Paxton, Physical Review B **40**, 3616 (1989).
[48] P. B. Allen and R. Dynes, Physical Review B **12**, 905 (1975).
[49] Z. C. Guo, F. Luo, and Y. Cheng, Computational Materials Science **84**, 139 (2014).
[50] C. J. Pickard and R. J. Needs, Nature Physics **3**, 473 (2007).
[51] R. F. Bader, Atoms in molecules: a quantum theory. international series of monographs on chemistry **22** (1990).
[52] P. B. Allen and B. Mitrović, Solid State Physics **37**, 1 (1983).